

Received 2 October 2024, accepted 8 November 2024, date of publication 14 November 2024, date of current version 9 December 2024.

Digital Object Identifier 10.1109/ACCESS.2024.3498448

RESEARCH ARTICLE

Improving Communication Signal Transmission in Multiple Low-e Windows Using Frequency Selective Surfaces

ROCIO CHUECA¹, (Associate Member, IEEE), MARIA MUÑOZ¹, ANA CUEVA², RAUL ALCAIN³, CARLOS D. HERAS¹, AND IÑIGO SALINAS¹

¹Instituto de Investigación en Ingeniería de Aragón (I3A), Universidad de Zaragoza, 50009 Zaragoza, Spain

²Facultad de Ciencias, Universidad de Zaragoza, 50009 Zaragoza, Spain

³Ariño Duglass, 50171 Zaragoza, Spain

Corresponding author: Rocio Chueca (rchueca@unizar.es)

This work was supported by the Fondo Europeo de Desarrollo Regional (FEDER)/Ministry of Science, Innovation and Universities—State Research Agency under Project RTC2019-007368-3 and Project CPP2022-010053.

ABSTRACT The use of low-emissivity and solar control glass for thermal insulation in transportation and architecture poses a problem for communications, since the metallic coatings used in this glass attenuate radiofrequency (RF) signals. One solution to this problem is to define Frequency Selective Surfaces (FSS) on the coatings to ensure the transmission of RF signals while maintaining the thermal properties of the glazing. On windows with multiple coated panes, the interaction between the different surfaces grows more complex, as the dimensions of the structure are in the order of the wavelength of the signals involved. This is also an opportunity for the design of windows with specific transmission properties. The aim of this work is to present a design method for windows with multiple low-e coatings and multiple FSS based on the optimization of the RF transmission using an equivalent transmission line model. As a validation of our method, we show designs for windows with attenuation minima at 1, 1.8 and 5.8 GHz. Window samples according to these designs have been fabricated and measured, showing good correlation between simulation and experiment.

INDEX TERMS Frequency selective surface (FSS), low-emissivity, glass, multilayer.

I. INTRODUCTION

The use of glass with thermal properties (both low-emissivity and solar control glass) is becoming increasingly common in both architecture and transportation. These glasses are characterised either by a transmission coefficient in the infrared spectrum much lower than that of conventional glasses (solar control glasses) or by an emissivity in the infrared spectrum very low, in order to avoid heat radiation into or out of a room (low-emissivity glasses) [1], [2], [3], [4], [5], [6]. Both effects are achieved by the deposition of a coating with at least one metallic layer on the glass. However, these metallic layers produce great attenuation -in the order of 40-50 dB [7]- at the frequencies used for wireless communications such as Wi-Fi, 3G, 4G or 5G. This will result

in loss of signal inside a building with a large glazing surface or a metallic vehicle such as a train.

There are different solutions to improve the RF transmission on low-e windows, as installing repeaters or the use of perimetally uncoated windows [8], [9], but the most common one is the use of frequency selective surfaces (FSS) [10], [11], [12], [13]. In these surfaces, usually metallic, periodic patterns are designed to transmit, reflect or absorb electromagnetic waves of a certain frequency range [14], [15]. If such patterns are defined in the metallic coatings of solar control or low-emissivity glass, different RF filters can be designed. The drawback is the loss of thermal efficiency of the coatings, which is directly dependent on the area of metallic layer removed.

When studying different FSS patterns significant differences in attenuation become evident when comparing a specific FSS pattern to the same FSS included in a complete

The associate editor coordinating the review of this manuscript and approving it for publication was Jon Atli Benediktsson¹.

window. If the wavelength of the electromagnetic wave passing through the window is in the order of the thickness of the glazing panes or gaps, resonances and interferences appear, leading to changes of amplitude in the transmitted and reflected waves. A multilayer model based on transmission line theory can be used to account for these effects and predict the performance of complex Insulating Glass Units (IGU), which may have multiple glass panes and gaps [16].

If the thermal efficiency requirements are very demanding, the IGU may contain multiple low-e coatings. An FSS must be defined in each of these coatings to ensure radio frequency signal transmission through the window, as the total attenuation in dB is the sum of the attenuation coefficients due to each coating.

The study of multi-pane windows with multiple FSS is a complex problem as, due to the presence of interference, it is not possible to simply add the effect of all the FSS. A method that can easily and quickly predict the RF transmission of a multi-pane IGU is essential for a design of these structures. These properties, such as letting through or blocking specific bands, can be of great interest for applications in both buildings and vehicles.

Structures with multiple FSS have been used in different applications as [17], [18], [19], [20], and [21] for multiple band response, reflectors [22], [23], wide band applications or absorbers [24]. As for multiple FSS applied to energy saving windows, there are some studies [25], [26], [27], [28], but they use complex and expensive simulation tools, as CST or ANSYS, to simulate the whole structure instead of a simple and fast model as is the transmission line theory. Also, the effect on thermal efficiency is not considered, and in most cases the simulations results are not contrasted with experimental measurements (Table 1).

Our study shows, through various design examples, how the transmission line model can be used to minimize the attenuation of RF signals at specific frequencies in the range of mobile communications (900-3500 MHz) for multi-pane windows with multiple FSS. The impact on heat transfer is also considered, and the results of the simulations are validated by measurements of samples fabricated according to the designs.

II. THEORETICAL MODEL

The proposed theoretical model for the IGU considers it as a multilayer structure with layers of different thicknesses d and impedances η . Every layer is a uniform, homogeneous and isotropic medium. The incident wave is a linearly polarized uniform plane wave. These assumptions make possible the use of transmission line theory, where each layer is equivalent to a section of transmission line of length equal to its thickness and with its same impedance. These lines can be considered lossless for the thicknesses involved (in the orders of millimeters), although the model can be easily updated to include losses.

The objective of this model (Figure 1) is to calculate the equivalent total impedance (Z_{if}) of the structure. For this

TABLE 1. Summary of studies using multiple FSS.

Ref.	Freq (MHz)	Field	Multilayer model	Thermal Study																																		
[17]	8-12	Reflectors	No	No																																		
[18]	10-12.4	Reflectors	No	No																																		
[19]	12-18	Reflectors	No	No																																		
[20]	5-25	Reflectors	No	No																																		
[21]	7-12	Reflectors	No	No																																		
[22]	3-15	Reflectors	No </tr <tr> <td>[23]</td> <td>4-7</td> <td>Reflectors</td> <td>No</td> <td>No</td> </tr> <tr> <td>[24]</td> <td>2-12</td> <td>Absorbers</td> <td>Yes</td> <td>No</td> </tr> <tr> <td>[25]</td> <td>0.5-2</td> <td>Low-e coating</td> <td>No</td> <td>No</td> </tr> <tr> <td>[26]</td> <td>0.8-6</td> <td>Low-e coating</td> <td>No</td> <td>No</td> </tr> <tr> <td>[27]</td> <td>0.6-2</td> <td>Low-e coating</td> <td>No</td> <td>No</td> </tr> <tr> <td>[28]</td> <td>0.9-6</td> <td>Low-e coating</td> <td>No</td> <td>No</td> </tr> <tr> <td>This study</td> <td>0.6-6</td> <td>Low-e coating</td> <td>Yes</td> <td>Yes</td> </tr>	[23]	4-7	Reflectors	No	No	[24]	2-12	Absorbers	Yes	No	[25]	0.5-2	Low-e coating	No	No	[26]	0.8-6	Low-e coating	No	No	[27]	0.6-2	Low-e coating	No	No	[28]	0.9-6	Low-e coating	No	No	This study	0.6-6	Low-e coating	Yes	Yes
[23]	4-7	Reflectors	No	No																																		
[24]	2-12	Absorbers	Yes	No																																		
[25]	0.5-2	Low-e coating	No	No																																		
[26]	0.8-6	Low-e coating	No	No																																		
[27]	0.6-2	Low-e coating	No	No																																		
[28]	0.9-6	Low-e coating	No	No																																		
This study	0.6-6	Low-e coating	Yes	Yes																																		

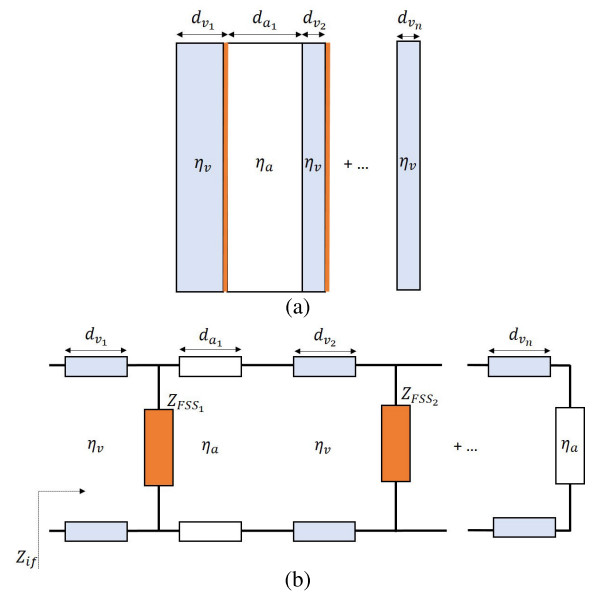


FIGURE 1. Multiglazed window (a) and its equivalent multilayer model.

purpose, and using expression (1), the intermediate equivalent impedances are calculated sequentially from right to left. In this case, there are two different types of layers, air and glass. Air layers (in white) have a well known impedance $\eta_0 = 120\pi$ whereas glass layers (in blue) have $\eta_v = \frac{\eta_0}{n_v}$, with $n_v = 2.65$ the refractive index of the glass for our frequency range. The metallic coatings, which include an FSS, (in orange) will be represented as impedances

in parallel.

$$Z_i = R_0 \frac{Z_L + jR_0 \tan \beta l}{R_0 + jZ_L \tan \beta l} = \eta_v \frac{\eta_0 + j\eta_v \tan \beta d_{v_n}}{\eta_v + j\eta_0 \tan \beta d_{v_n}} \quad (1)$$

Once Z_i is calculated for the rightmost layer, the process is repeated until the total impedance of the window Z_{if} is obtained (2). Then, the global reflection coefficient Γ can be calculated (3) and, from it, the power transmission coefficient T and the attenuation of the structure.

$$Z_{if} = \eta_v \frac{Z_{i_{n-1}} + j\eta_v \tan \beta d_{v_1}}{\eta_v + jZ_{i_{n-1}} \tan \beta d_{v_1}} \quad (2)$$

$$\Gamma = \frac{Z_{if} - \eta_0}{Z_{if} + \eta_0} \rightarrow T = 1 - |\Gamma|^2 \quad (3)$$

$$Att(dB) = -10 \log_{10}(T) \quad (4)$$

These equations are only valid for normal incidence and need to be modified to include different angles of incidence θ , which can be accomplished simply by modifying the values of the thicknesses and impedances of the different layers. If we consider TE waves as those with an E-field perpendicular to the plane of incidence (perpendicular polarization), and TM waves as those in which the E-field is in the plane of incidence (parallel polarization), the equivalent impedances of a layer are,

$$\eta_i^{TE}(\theta) = \frac{\eta_i}{\cos \theta} \quad \eta_i^{TM}(\theta) = \eta_i \cos \theta \quad (5)$$

and the equivalent thickness for an angle of incidence θ ,

$$d_i^{TE, TM}(\theta) = d_i \cos \theta \quad (6)$$

A. FSS

The impedance of a FSS can take different values depending on its design. In this study we will use only two of the more common structures, patch and mesh (Figure 2).

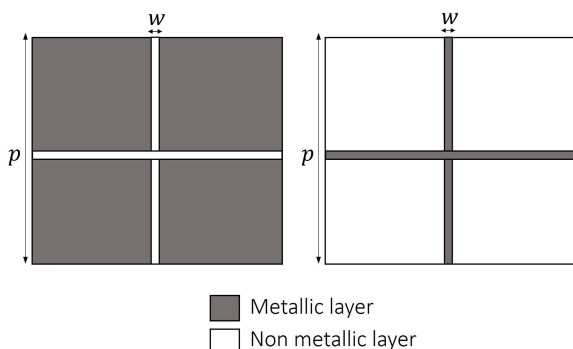


FIGURE 2. Patch (left) and mesh (right) FSS pattern.

The mesh pattern consists of vertical and horizontal metallic lines of the same thickness and periodicity. When the electric field is parallel to the lines, a current is induced and the FSS behaves as an inductor with $Z_{FSS} = j\omega L_{FSS}$, and will work as a high pass filter. The lines transversal to the electric field will define capacitors but, if $p \gg w$, this capacitance

will usually be negligible. As there are vertical and horizontal lines, these assumptions will be valid for both polarizations. The expressions for the impedance of the inductors can be obtained from [29],

$$L_{FSS}^{TE} = \frac{p\mu_0}{2\pi} \ln \left(\frac{1}{\sin(\frac{\pi w}{2p})} \right) \quad (7)$$

$$L_{FSS}^{TM} = L_{FSS} \left(1 - \frac{k_0^2 \sin^2(\theta)}{2k_{eff}^2} \right) \quad (8)$$

The patch pattern is obtained by removing the metallic coating along vertical and horizontal lines of the same thickness (w) and periodicity (p). In this case, the lines transversal to the electric field will again be equivalent to capacitors and the conducting patches to inductors, but now the capacitance will be much larger and thus the FSS impedance similar to that of a capacitor $Z_{FSS} = \frac{j}{\omega C_{FSS}}$, resulting in a low pass filter. The equivalent capacitances can be obtained using Babinet's principle:

$$C_{FSS}^{TM} = \frac{p\epsilon_0(\epsilon_{r1} + \epsilon_{r2})}{\pi} \ln \left(\frac{1}{\sin(\frac{\pi w}{2p})} \right) \quad (9)$$

$$C_{FSS}^{TE} = C_{FSS} \left(1 - \frac{k_0^2 \sin^2(\theta)}{2k_{eff}^2} \right) \quad (10)$$

These expressions are valid if the FSS periodicity is smaller than a half-wavelength [29], which is true for our measurement range and FSS dimensions.

The multilayer model can be used to formulate a design method for different window structures. These windows can be single, double or multi-glazed and can have coatings with FSS in one or more of their panes. One way of designing a window with FSS is to obtain an attenuation null for a specific frequency. Per the transmission line model, this is equivalent to achieving a reflection coefficient $\Gamma = 0$, which occurs when the input impedance of the circuit is matched to the reference impedance (in this case the impedance of the air, $\eta_a = \eta_0$). The matching condition (or conditions) provide a set of equations from which the values of Z_{FSS_n} can be determined.

B. OPTICAL AND THERMAL PROPERTIES

The thermal transmission coefficient (U), according to the UNE-673 standard [30], is a widely used parameter [31], [32] that evaluates the amount of heat that passes through the glazing per unit area. The units are watts per square metre and degree Kelvin (W/m^2K). This value is defined by the following expression:

$$\frac{1}{U} = \frac{1}{h_e} + \frac{1}{h_t} + \frac{1}{h_i} \quad (11)$$

h_e is the external heat transfer, h_t is the total heat transfer and h_i is the internal heat coefficient.

The external heat transfer coefficient h_e is a function of wind speed near the glazing, emissivity and other climatic

factors. For ordinary vertical glazing, the value of h_e is standardised to $25 \text{ W}/(\text{m}^2 \cdot \text{K})$.

Additionally, the internal heat transfer coefficient (h_i) is:

$$h_i = h_c + h_r = 3.6 + \frac{4.4\epsilon}{0.837} \quad (12)$$

where ϵ is the corrected emissivity of the surface coated by a layer and 0.837 is the corrected emissivity of the ordinary glass.

The total heat transfer equation h_t is given by:

$$\frac{1}{h_t} = \sum_1^N \frac{1}{h_s} + \sum_1^M d_j r_j \quad (13)$$

h_s is the thermal conductance of each gas layer, N is the number of gas layers, d_j is the thickness of each material layer, r_j is the thermal resistivity of each material and M is the number of material layers. We can calculate the thermal conductance of a layer as:

$$h_s = h_r + h_g \quad (14)$$

where h_r is the radiative thermal conductance of the gas film and h_g is the thermal conductance of the gas.

The conductance due to radiation (h_r) is given by the formula:

$$h_r = 4\sigma \left(\frac{1}{\epsilon_1} + \frac{1}{\epsilon_2} - 1 \right)^{-1} T_m^3 \quad (15)$$

σ is the Stefan-Boltzman constant, T_m is the mean absolute temperature of the gas layer and ϵ_1 and ϵ_2 are the emissivities adjusted to the temperature T_m .

The gas conductance h_g is given by the formula:

$$h_g = Nu \frac{\lambda}{s} \quad (16)$$

where $Nu = A(GrPr)^n$, s is the thickness of the sheet and λ is the thermal conductivity.

$$Gr = \frac{9.81 s^3 \Delta T \rho^2}{T_m \mu} \quad (17)$$

$$Pr = \frac{\mu c}{\lambda} \quad (18)$$

where ΔT is the temperature difference between the glass surfaces on either side of the gas chamber, ρ is the density, μ is the dynamic viscosity, c is the mass thermal capacity.

In our case, the chambers of the multi glazed windows are filled with air, the climatic conditions are standard and the position of the glazing is vertical. For this conditions, these values of these parameters are (Table 2):

TABLE 2. Values for chambers filled with air and standard climatic conditions.

$\rho(\text{kg}/\text{m}^3)$	$\mu(\text{kg}/\text{ms})$	$\lambda(\text{W}/\text{mK})$	$c(\text{J}/\text{kgK})$	$T_m(\text{K})$
1.232	1.76e-6	0.02496	1008	283
$\Delta T(\text{K})$	$h_e(\text{W}/\text{m}^2\text{K})$	$h_i(\text{W}/\text{m}^2\text{K})$	A	n
15	25	8	0.035	0.38

In the case of a pane with an FSS, the only difference is the emissivity of the surface in equation (12), which can be calculated as:

$$\epsilon_{total} = \frac{Area_{glass}}{Area_{total}} \epsilon_{glass} + \% \frac{Area_{coating}}{Area_{total}} \epsilon_{coating} \quad (19)$$

III. MULTI-PANE WINDOWS DESIGNS

In order to understand properly the RF properties and the thermal behaviour of multi-pane windows with FSS, it is important to consider how these glazings behave, both with or without the full low-e coating (Figure 3).

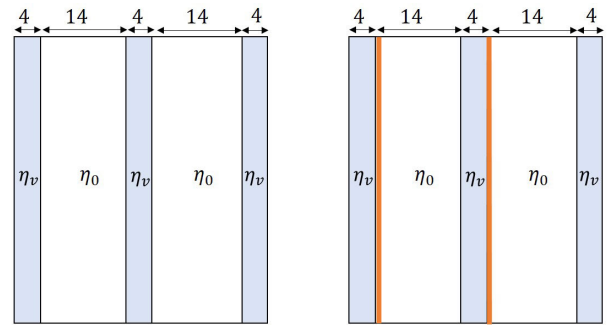


FIGURE 3. Reference triple glazed windows: without coating (left) and double low-e coating (right).

Our reference triple glazed window is formed by three monolithic glasses and two air chambers. To improve the performance of the IGU, a metallic coating can be deposited on the second face of the first two glasses (i.e., face 2 and 4). In this case, both gaps are 14 mm in width and the glass panes are 4 mm thick. The attenuation is not constant along the range of frequencies of interest due to the resonances produced in the different surfaces of the window. If two low-e coatings are added to this same window, the attenuation is near 80 dB.

To calculate the U-factor for both windows, we need the emissivity of the glass and the low-e coating, which for our samples will be 0.837 and 0.028. Using this values and the parameters and equations of the previous section, the U-factor of the triple glazed window is 1.831 without low-e coating and decreases to 0.820 with the double coating.

If we define FSS in the low-e coatings, the emissivity changes and, with it, the U-factor. The emissivity of the FSS used in this study are calculated using the equation 19 and listed in Table 3.

TABLE 3. Emissivity of a 0.028 low-e coating with different FSS.

Glass sample	% Layer removed	Emissivity (ϵ)
FSS p = 2 mm	10	0.109
FSS p = 3 mm	6.6	0.082
FSS p = 15 mm	1.3	0.038

A. TRIPLE GLAZED WINDOW WITH AN ATTENUATION MINIMUM AT 1.8 GHz

In this example we use a triple glazed window with two low-e coatings, as shown in Figure 3. The width of the glazing gaps is 14 mm. We search for an attenuation minimum at 1.8 GHz, as it is a frequency shared by 2G and 4G and thus, convenient to let it pass through windows both in buildings and vehicles. In this case, the matching condition $\Gamma = 0$ results in values for the capacitors of 0.115 pF and 0.252 pF and, therefore, patch FSS with w of 100 μm and p of 2 and 3 mm. The attenuation (Figure 4) remains under 10 dB up to 3.5 GHz, although there are changes in the position of the minimum for large incidence angles, especially in the case of the TM polarization.

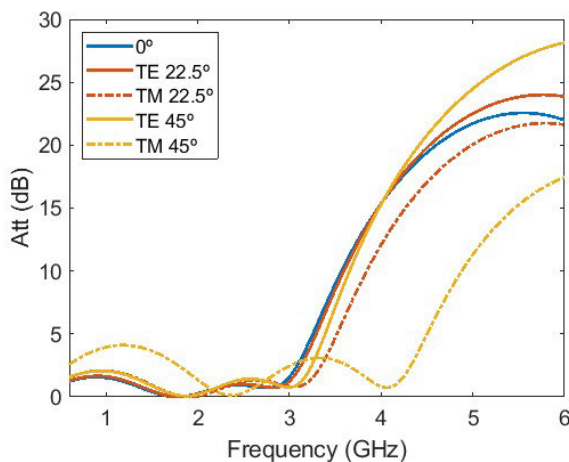


FIGURE 4. Simulated attenuation (dB) for TE and TM polarization of a triple glazed window with min att. at 1.8 GHz.

The other solution for the equivalent circuit for this configuration requires very small values for the capacitors (6.69 and 27.7 fF), equivalent to patch FSS of p 0.35 and 0.75 mm. Although this solution is also valid, the amount of coating that should be removed (40% and 22%) makes it impractical, as the window would lose almost most of its thermal insulation. Therefore, this solution will not be taken into account.

This window with two FSS can then be compared to the reference windows introduced before, the uncoated triple glazed and the fully low-e coated triple glazed window (Figure 5). The attenuation for the low-e window with FSS is as low or even lower than the attenuation of the window without low-e coatings around 1.8 GHz, as intended in our design. This low attenuation region extends up to 3GHz, where the attenuation starts to rise, although is still far from the near 80dB of the fully coated window. The usual limits for the attenuation of a commercial low-e window with FSS are between 10 and 15 dB, so this design would be valid up to 3.5-4 GHz.

Regarding the thermal properties of this example, the U-factor is equal to 0.938, up but close to the original value of 0.820 with the full coating.

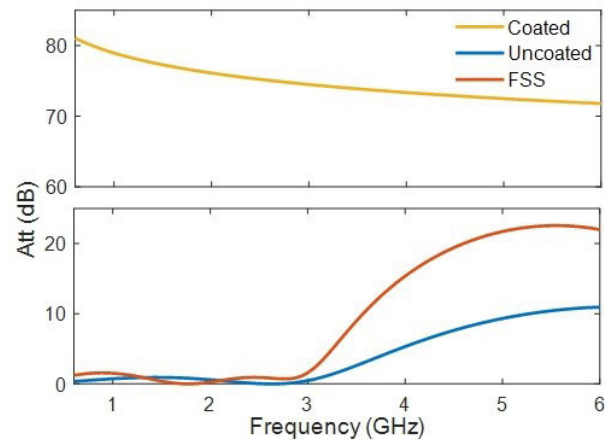


FIGURE 5. Comparison of a triple glazed window with FSS of $p = 2$ and $p = 3$ mm, uncoated window and double coated window.

B. TRIPLE GLAZED WINDOW WITH A MINIMUM AT 1 GHz

This is a window designed to work at the lowest frequency bands for mobile communication and, at the same time, stop signals in the Wi-Fi bands (2.4 and 5 GHz). Therefore, we solve the equivalent circuit using impedance matching to find an attenuation minimum at 1 GHz while the attenuation at 2.4 GHz remains over 20 dB. In this case, both FSS are patch patterns of $w = 100\mu\text{m}$ and $p = 15$ mm, equivalent to capacitors of 1.65 pF. The attenuation for different incident angles and polarizations is shown in Figure 6.

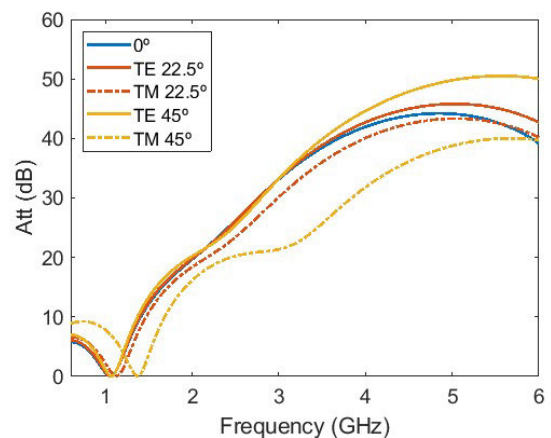


FIGURE 6. Simulated attenuation (dB) for TE and TM polarization of a triple glazed window with min att. at 1 GHz.

Figure 7 shows how the double low-e window with FSS achieves the desired result of an attenuation minimum near 1GHz, which increases up to 40 dB to reject the Wi-Fi signals. Here the selective surfaces are not used only to minimize the effect of the low-e coatings, but to obtain advanced RF properties which are not possible with the uncoated window.

Moreover, this design maintains the insulation performance of the standard double low-e coated window. The U-factor for this IGU is 0.849, very close to the original value of 0.820.

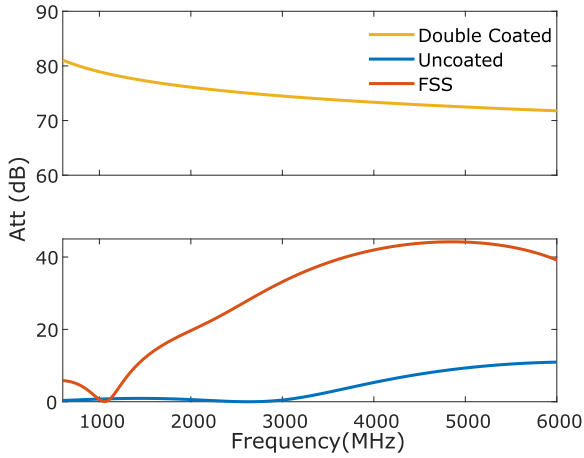


FIGURE 7. Comparison of a triple glazed window with 2 FSS of $p = 15$ mm, uncoated window and double coated window.

IV. HIGH EMISSIVITY FSS

Once our model has been presented and used in the design of different triple glazed windows, it is easy to apply this design method to different configurations.

A double glazed window can be formed by a laminated glass (in our case two 4 mm glass panes separated by a butyral sheet 1.5 mm thick), an air gap (15 mm) and a third glass pane (5 mm). If necessary, the low-e coating is deposited on the face after the laminated glass (i.e, face 2). Both windows are shown in Figure 8.

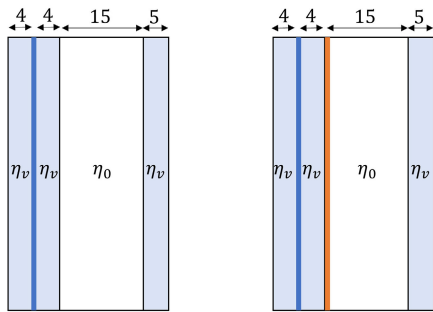


FIGURE 8. Reference double glazed windows: uncoated (left) and low-e coated (right).

The U-factor for the double glazed window without low-e coating is 2.688 and 1.353 for the low-e window. The RF attenuation of the low-e window is near 40 dB.

As the standard low-e double glazed window has just one low-e coating, it only admits one FSS. However, an additional metallic coating can be placed on the third pane in order to add another FSS and, with it, further RF transmission design possibilities. One of those possibilities is to achieve a minimum of attenuation at the 5 GHz band, used in both Wi-Fi and 5G networks. This condition is very difficult to obtain using only patch FSS, as the usual dimensions of the air gap result in a resonance (and an attenuation maximum) in the 4-6 GHz range.

A. DOUBLE GLAZED WINDOW WITH A MINIMUM AT 5.8 GHz

The upper bands used in 5G communications (in the 5-7 GHz range) present an interesting challenge for the design of FSS low-e windows, as the usual structure of the window itself (the thickness and spacing between the glass panes) produces a resonance that contributes to the rise of the attenuation in that region. The dimensions of the structure cannot be easily changed due to design constraints in buildings and vehicles, but the use of multiple FSS provides additional degrees of freedom to achieve the desired attenuation levels.

As an example of this, the solution to achieve the matching condition $\Gamma = 0$ in 5.8 GHz is to use two FSS, one of them inductive (mesh pattern). This design will be valid for windows needing only one coated surface for thermal insulation, as the thermal contribution of the coating with the mesh FSS will be minimal. This is due to the large surface of coating removed, which will result in high emissivity for that pane, almost the same of the uncoated glass. The equivalent circuit model is shown in Figure 9.

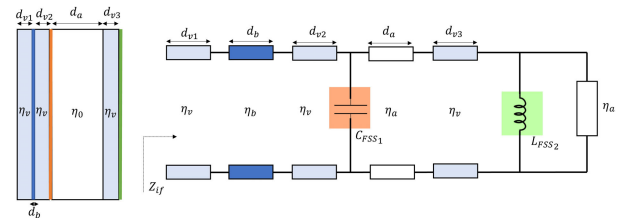


FIGURE 9. Double glazed window with two FSS, capacitive and inductive.

The design for an attenuation minimum at 5.8 GHz results in a double glazed unit like that of Figure 9 with a patch FSS ($p = 5$ mm and $w = 100\mu m$), an air chamber of 15 mm and a third 4 mm glass with a mesh FSS ($p = 5$ mm and $w = 1$ mm). The equivalent capacitor is $C = 0.46$ pF and the inductor is $L = 1.14$ nH. The emissivities of each glass with the different FSS patterns are listed in Table 4

TABLE 4. Emissivity of the glass panes with FSS used in the window.

Glass sample	% Layer removed	Emissivity (ϵ)
Grid $p = 5$ mm $w = 1$ mm	64	0.545
Patch $p = 5$ mm $w = 100$ um	4	0.060

The U-factor of our design is equal to 1.443, very similar to the value of 1.353 for the conventional window with one fully low-e coated surface. This shows that we can design an IGU with tailored RF transmission properties without changing its thermal insulation properties.

V. EXPERIMENTAL SET-UP AND RESULTS

The experimental set-up, placed in an anechoic chamber, uses two 600 MHz - 6 GHz Vivaldi antennas (RFSpace TSA600) and a picoVNA 106 vector network analyzer. A metal plate around the windows will ensure that only the

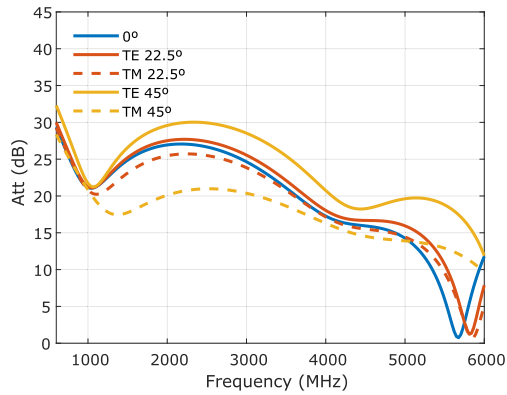


FIGURE 10. Simulated attenuation (dB) for TE and TM polarization of a double glazed window with a minimum of attenuation at 5 GHz.

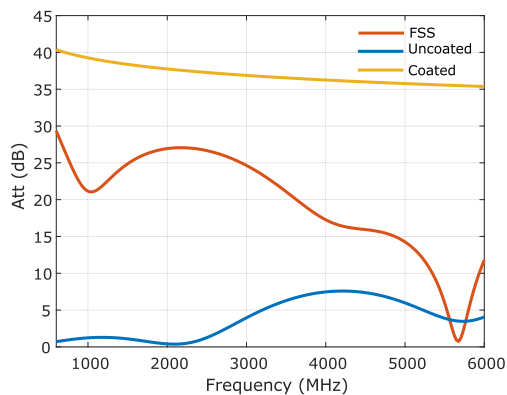


FIGURE 11. Comparison of our design to the same window without low-e coating and with one low-e coated glazing.

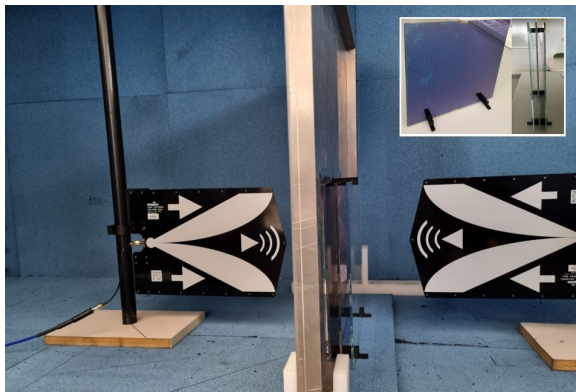


FIGURE 12. Experimental set-up and window sample.

signal passing through the windows reaches the reception antenna (Figure 12).

The measurement of the power transmitted through the window sample is referenced to the power transmitted when the setup holds no samples to obtain the attenuation of the window. The prototypes were fabricated using glass panes with and without low-e coating and the adequate spacers to simulate the gaps between panes. The low-e coating is deposited by sputtering. The samples were measured for

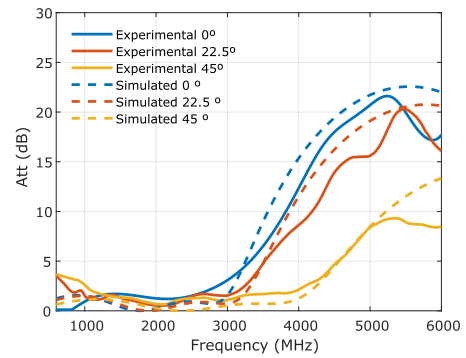
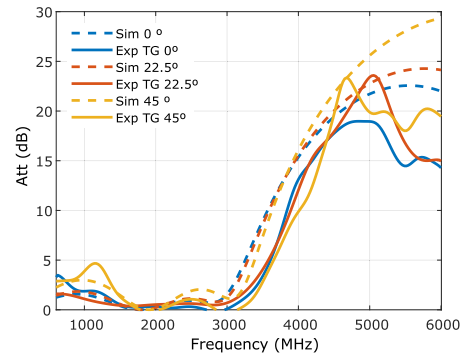


FIGURE 13. Attenuation of a triple glazed window with 2 patch FSS of $p_1 = 2 \text{ mm}$ and $p_2 = 3 \text{ mm}$ for TE polarization (a) and TM polarization (b).

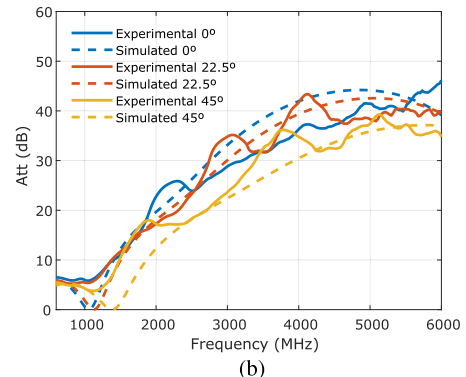
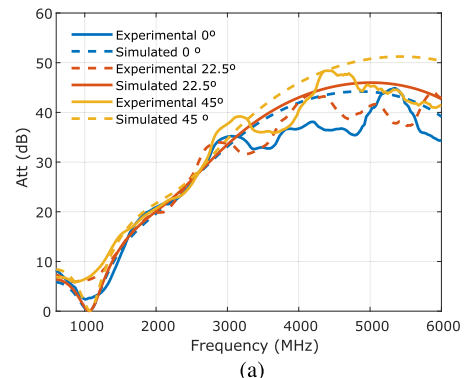


FIGURE 14. Attenuation of a triple glazed window with 2 patch FSS of $p = 15 \text{ mm}$ for TE polarization (a) and TM polarization (b).

both polarizations (TE and TM) and for different angles of incidence: 0° , 22.5° and 45° .

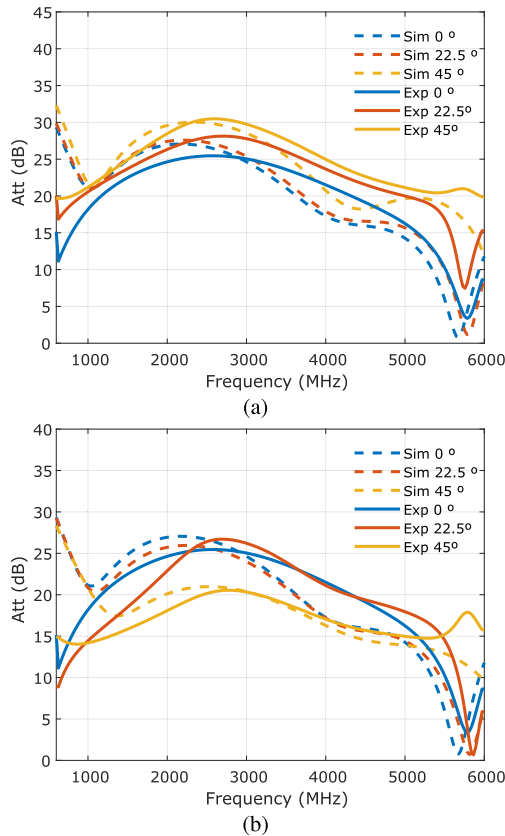


FIGURE 15. Attenuation of a triple glazed window with 1 patch FSS of $w = 0.1 \text{ mm}$ and $p = 5 \text{ mm}$ and 1 mesh FSS of $w = 1 \text{ mm}$ and $p = 5 \text{ mm}$ for TE polarization (a) and TM polarization (b).

The experimental results for the first window are compared to the simulation in Figure 13a and 13b. The measurements are in good accordance with the simulation, although the deviation is larger for the ranges with higher attenuation, as the impact of the quality of the chamber absorbers is much more noticeable when measuring weaker signals. This window has very low attenuation in the design range and will be a good alternative for applications where an attenuation of less than 10dB up to 3.5GHz is desired.

The second of the windows simulated in the previous section has also been fabricated. There is again a good match between simulation and experiment and, as desired, the attenuation remains low around 1 GHz and increases to 25 dB at 2.4 GHz and 40 dB at 5 GHz to block Wi-Fi signals.

The results of the third window are shown in Figure 15. As in the previous samples, the experimental results match the theoretical model for both polarizations and different angle of incidence.

VI. CONCLUSION

In this study, a design method for multi-pane windows with multiple low-e coatings and frequency selective surfaces has been presented. With this method, it is possible to find a minimum of attenuation for specific frequencies using multiple glass panes and air gaps and patch (capacitive) or mesh (inductive) FSS.

The thermal transmission coefficient (U) of the different window designs is studied and evaluated. Patch FSS have low impact on the U-factor, as the surface of the low-e coating removed is quite small. That is not the case for mesh FSS, but they can still be used if an additional low-e coating, useful only for its RF transmission properties and not as a thermal insulator, is included in the IGU.

The simulation and design method has been validated by comparison to measurements of different samples in an anechoic chamber, with good agreement between simulation and experiment.

This is a simple and fast technique to design complex windows with custom RF properties for different applications in architecture and transportation.

REFERENCES

- [1] A. Karttunen, M. Mökkönen, and K. Haneda, "Investigation of 5G radio frequency signal glazing structures," *Glass Performance Days*, Jun. 2019.
- [2] S. Xie, Z. Ji, L. Zhu, J. Zhang, Y. Cao, J. Chen, R. Liu, and J. Wang, "Recent progress in electromagnetic wave absorption building materials," *J. Building Eng.*, vol. 27, Jan. 2020, Art. no. 100963.
- [3] C. Schaefer, G. Bräuer, and J. Szczyrbowski, "Low emissivity coatings on architectural glass," *Surf. Coatings Technol.*, vol. 93, no. 1, pp. 37–45, Aug. 1997.
- [4] A. Asp, Y. Sydorov, M. Valkama, and J. Niemelä, "Radio signal propagation and attenuation measurements for modern residential buildings," in *Proc. IEEE Globecom Workshops*, Dec. 2012, pp. 580–584.
- [5] I. Rodríguez, H. C. Nguyen, N. T. K. Jorgensen, T. B. Sorensen, and P. Mogensen, "Radio propagation into modern buildings: Attenuation measurements in the range from 800 MHz to 18 GHz," in *Proc. IEEE 80th Veh. Technol. Conf. (VTC-Fall)*, Sep. 2014, pp. 1–5.
- [6] B. P. Jelle, S. E. Kalnaes, and T. Gao, "Low-emissivity materials for building applications: A state-of-the-art review and future research perspectives," *Energy Buildings*, vol. 96, pp. 329–356, Jun. 2015.
- [7] P. Ragulis, P. Ångskog, R. Simiškiš, B. Vallhagen, M. Bäckström, and Ž. Kancleris, "Shielding effectiveness of modern energy-saving glasses and windows," *IEEE Trans. Antennas Propag.*, vol. 65, no. 8, pp. 4250–4258, Aug. 2017.
- [8] H. Kim and S. Nam, "Transmission enhancement methods for low-emissivity glass at 5G mmWave band," *IEEE Antennas Wireless Propag. Lett.*, vol. 20, no. 1, pp. 108–112, Jan. 2021.
- [9] R. Chueca, R. Alcain, C. Heras, and I. Salinas, "Radiofrequency transmission through rectangular apertures in perimetally uncoated low emissivity windows," *J. Phys. D, Appl. Phys.*, vol. 57, no. 8, Feb. 2024, Art. no. 085103.
- [10] L. Burnier, M. Lanini, O. Bouvard, D. Scanferla, A. Varathan, C. Genoud, A. Marguerit, B. Cattat, N. Dury, R. Witte, A. Salvadè, and A. Schüller, "Energy saving glazing with a wide band-pass FSS allowing mobile communication: Up-scaling and characterisation," *IET Microw., Antennas Propag.*, vol. 11, no. 10, pp. 1449–1455, Aug. 2017.
- [11] R. Chueca, R. Alcain, C. Heras, and I. Salinas, "Modelling of frequency selective surfaces on multi-layered glazing windows," in *Proc. Global Conf. Wireless Opt. Technol. (GCWOT)*, Feb. 2022, pp. 1–5.
- [12] L. Yunos, M. L. Jane, P. J. Murphy, and K. Zuber, "Frequency selective surface on low emissivity windows as a means of improving telecommunication signal transmission: A review," *J. Building Eng.*, vol. 70, Jul. 2023, Art. no. 106416.
- [13] G. I. Kiani, S. Habib, M. F. U. Butt, and A. J. Aljohani, "RF/MW transmission improvement in energy efficient buildings using FSS and its impact on thermal efficiency of energy-saving glass," *J. Electron. Mater.*, vol. 52, no. 11, pp. 7525–7533, Nov. 2023.
- [14] B. A. Munk, *Finite Antenna Arrays and FSS*. Hoboken, NJ, USA: Wiley, 2003.
- [15] B. A. Munk, *Frequency Selective Surfaces: Theory and Design*. Hoboken, NJ, USA: Wiley, 2005.
- [16] J. R. Wait, *Electromagnetic Waves in Stratified Media: Revised Edition Including Supplemented Material*, vol. 3. Amsterdam, The Netherlands: Elsevier, 2013.

[17] D. Zelenchuk and V. Fusco, "Split-ring FSS spiral phase plate," *IEEE Antennas Wireless Propag. Lett.*, vol. 12, pp. 284–287, 2013.

[18] S. Kumar, L. Kurra, M. Abegaonkar, A. Basu, and S. K. Koul, "Multilayer FSS for gain improvement of a wide-band stacked printed antenna," in *Proc. Int. Symp. Antennas Propag. (ISAP)*, Nov. 2015, pp. 1–4.

[19] A. Chatterjee and S. K. Parui, "A multi-layered band-pass frequency selective surface designed for Ku band applications," in *Proc. IEEE Appl. Electromagn. Conf. (AEMC)*, Dec. 2013, pp. 1–2.

[20] M. Yan, J. Wang, H. Ma, M. Feng, Y. Pang, S. Qu, J. Zhang, and L. Zheng, "A tri-band, highly selective, bandpass FSS using cascaded multilayer loop arrays," *IEEE Trans. Antennas Propag.*, vol. 64, no. 5, pp. 2046–2049, May 2016.

[21] A. L. P. S. Campos, R. H. C. Maniçoba, L. M. Araújo, and A. G. d'Assunção, "Analysis of simple FSS cascading with dual band response," *IEEE Trans. Magn.*, vol. 46, no. 8, pp. 3345–3348, Aug. 2010.

[22] Y. Ranga, L. Matekovits, K. P. Esselle, and A. R. Weily, "Multilayer frequency-selective-surface reflector for constant gain over ultra wide-band," in *Proc. 5th Eur. Conf. Antennas Propag. (EUCAP)*, Apr. 2011, pp. 332–334.

[23] A. Chatterjee and S. K. Parui, "A dual layer frequency selective surface reflector for wideband applications," *Radioengineering*, vol. 25, no. 1, pp. 67–72, Apr. 2016.

[24] Z. Yao, S. Xiao, Y. Li, and B.-Z. Wang, "On the design of wideband absorber based on multilayer and multiresonant FSS array," *IEEE Antennas Wireless Propag. Lett.*, vol. 20, no. 3, pp. 284–288, Mar. 2021.

[25] S. I. Sohail, K. P. Esselle, and G. Kiani, "Design of a bandpass FSS on dual layer energy saving glass for improved RF communication in modern buildings," in *Proc. IEEE Int. Symp. Antennas Propag.*, Jul. 2012, pp. 1–2.

[26] F. Ma and L. Li, "Design of a tri-bandpass FSS on dual-layer energy saving glass for improving RF transmission in green buildings," in *Proc. IEEE Int. Conf. Commun. Problem-Solving (ICCP)*, Oct. 2015, pp. 405–407.

[27] G. I. Kiani and R. W. Aldhaheri, "Wide band FSS for increased thermal and communication efficiency in smart buildings," in *Proc. IEEE Antennas Propag. Soc. Int. Symp. (APSURSI)*, Jul. 2014, pp. 2064–2065.

[28] F. Bagci, C. Mulazimoglu, S. Can, E. Karakaya, A. E. Yilmaz, and B. Akaoglu, "A glass based dual band frequency selective surface for protecting systems against WLAN signals," *AEU-Int. J. Electron. Commun.*, vol. 82, pp. 426–434, Dec. 2017.

[29] F. Costa, A. Monorchio, and G. Manara, "An overview of equivalent circuit modeling techniques of frequency selective surfaces and metasurfaces," *Appl. Comput. Electromagn. Soc. J.*, vol. 29, no. 12, pp. 960–976, Dec. 2014.

[30] *UNE-EN 673/A1:2001 AENOR Glass Building. Determination Thermal Transmittance (U Value)-Calculation Method*, AENOR, 2001. [Online]. Available: <https://www.une.org/>

[31] S. Pal, B. Roy, and S. Neogi, "Heat transfer modelling on windows and glazing under the exposure of solar radiation," *Energy Buildings*, vol. 41, no. 6, pp. 654–661, Jun. 2009.

[32] M. Alwetaishi, "Impact of glazing to wall ratio in various climatic regions: A case study," *J. King Saud Univ.-Eng. Sci.*, vol. 31, no. 1, pp. 6–18, Jan. 2019.



MARIA MUÑOZ received the B.Sc. degree in telecommunications from the University of Zaragoza, Zaragoza, Spain, in 2023, where she is currently pursuing the M.Sc. degree in telecommunications. She joined the Photonics Technologies Group, Aragon Institute for Engineering Research (IA), University of Zaragoza, as a Researcher, in 2023, and work for several projects related to optics, electronics, solar energy, and radiofrequency.



ANA CUEVA received the degree in physics from the University of Zaragoza, Zaragoza, Spain, in 1997. She is currently a Personal Researcher with the Department of Applied Physics, University of Zaragoza, where she is also a member of the Engineering Research Institute of Aragon (I3A). Her research interest includes optical and electromagnetic property characterization of physical vapor deposition (PVD) thin films.



RAUL ALCAIN received the B.Sc. ad M.Sc. degrees in physics from the University of Zaragoza, Zaragoza, Spain, in 2017 and 2019, respectively. He is currently pursuing the Ph.D. degree with the Photonics Technologies Group. He joined the Photonics Technologies Group, Aragon Institute for Engineering Research (I3A), University of Zaragoza, as a Researcher, in 2017, and work for several projects. He started working on the Research Department of the glass company Arino Duglass, in 2021. His current research interests include radiofrequency transmission through energy saving windows that includes frequency selective surfaces, laser technology, metallic coatings, and RF measurements.



CARLOS D. HERAS received the M.Sc. degree in physics from the University of Zaragoza, in 1994, and the Ph.D. degree in physics studying optical fiber nonlinearities and their effects and applications in optical communications, in 2003. He began working with Cables de Comunicaciones, a Spanish company that manufactures optical cables and optical sensors as a Technician with the Optical Communications Laboratory. In 2004, he joined the University of Zaragoza as an

Assistant Professor. He became an Associate Professor, in 2008. He has been involved in several public and privately funded projects related to nonlinear optical fiber and telecom applications using high resolution spectroscopy. He is also a member of the Photonics Technology Group, University of Zaragoza, involved in several projects related to optical communications, solar renewable energy, frequency selective surfaces, RF measurements, and radar technology. He is member of the Aragon Institute of Engineering Research (I3A).



IÑIGO SALINAS received the M.Sc. and Ph.D. degrees in physics from the Sciences Faculty, University of Zaragoza, Spain, in 1996 and 2003, respectively. He is currently an Associate Professor with the Electrical Engineering and Communications Department, University of Zaragoza, and a member of the Photonics Technologies Group, Aragon Institute of Engineering Research (I3A). His main research interests include optical characterization instrumentation and multilayers and frequency selective surfaces on advanced properties glass.



ROCIO CHUECA (Associate Member, IEEE) received the B.Sc. degree in telecommunications and the M.Sc. degree in telecommunications engineering from the University of Zaragoza, Zaragoza, Spain, in 2017 and 2019, respectively. She is currently pursuing the Ph.D. degree with the Photonics Technologies Group. She joined the Photonics Technologies Group, Aragon Institute for Engineering Research (I3A), University of Zaragoza, as a Researcher, in 2017, and work for

several projects related to optics, electronics, solar energy and radiofrequency. Her current research interests include radiofrequency transmission through energy saving windows that includes frequency selective surfaces, electromagnetic simulations, periodic structures, and RF.

...